Photocatalytic treatment of 4-chlorophenol in aqueous ZnO suspensions: Intermediates, influence of dosage and inorganic anions

Umar Ibrahim Gaya [a], Abdul Halim Abdullah [a,b,*], Zulkarnain Zainal [a], Mohd Zobir Hussein [a,b]

[a] Department of Chemistry, Faculty of Science, Universiti Putra Malaysia, 43400 UPM Serdang, Selangor D.E., Malaysia
[b] Advanced Materials and Nanotechnology Laboratory, Institute of Advanced Technology, Universiti Putra Malaysia, 43400 UPM Serdang, Selangor D.E., Malaysia

ARTICLE INFO

ABSTRACT

The photocatalytically driven removal of eco-persistent 4-chlorophenol from water using ZnO is reported here. Kinetic dependence of transformation rate on operating variables such as initial 4-chlorophenol concentration and photocatalyst doses was investigated. A complete degradation of 4-chlorophenol at $50\,mg\,L^{-1}$ levels was realised in 3 h. Analytical profiles on 4-chlorophenol transformation were consistent with the best-line fit of the pseudo zero-order kinetics. The addition of small amounts of inorganic anions as SO_4^{2-}, HPO_4^{-}, $S_2O_8^{2-}$ and Cl^- revealed two anion types: active site blockers and rate enhancers. Fortunately, Cl^- and SO_4^{2-} commonly encountered in contaminated waters enhanced the rate of 4-chlorophenol degradation. The reaction intermediates and route to 4-chlorophenol mineralisation were elucidated by combined RP-HPLC and GC–MS methods. In addition to previously reported pathway products of 4-chlorophenol photo-oxidation catechol was detected. A radical mechanism involving o-hydroxylation is proposed to account for the formation of catechol.

1. Introduction

In recent years, attention has been paid globally to the eradication of hazardous materials from wastewaters [1,2]. Nowadays, a high number of contaminants are resistant to conventional treatment methods. Generally, the traditional methods of treatment may be non-destructive [3], slow at higher concentration [4] or rather ineffective at low contaminant levels. It is therefore crucial to develop newer technologies. Advanced oxidation technologies (AOTs) constitute a collection of established treatment methods which rely on the photogeneration of highly oxidising radical species to effect the destruction of persistent pollutants. For over two decades, heterogeneous photocatalytic AOT is placed in the forefront of vigorous research activity due to its efficiency of total destruction of pollutants, non-selectivity and formation of benign products.

Photocatalytic oxidation technology exploits photoactivated semiconductors to degrade low levels of contaminants in both air and water. TiO$_2$ is the chief semiconductor used owing to its inertness (chemically and biologically), efficiency, cost effectiveness and ready availability [5–8]. However, the extensive use of TiO$_2$ is uneconomical for large-scale water treatment. Given the

drawbacks to the application of titania in the waste remediation, there is renewed interest to search for more reliable photocatalysts. ZnO exhibits comparatively analogous attributes and versatility to TiO$_2$. ZnO has nearly the same band gap energy and follows the same mechanism of photodegradation as TiO$_2$. In fact ZnO is considered as a suitable alternative to TiO$_2$, sometimes ranked higher in photocatalytic performance [9,10].

Chlorophenols constitute a group of serious environmental pollutants that must be eliminated. As a result of their widespread use in mothproofing, miticides, pesticides, herbicides, germicides, fungicides and wood preservation, chlorophenols pose a serious threat to the environment. Chlorophenols can be found in surface water, soil and industrial water [11–13]. The US EPA consolidated list of chemicals contains inter alia several chlorophenols under the Emergency Planning and Community Right-To-Know (EPRC) section. 4-Chlorophenol has direct relevance to water remediation due to its solubility and the severity of hazard to both terrestrial and aquatic life [14–17]. 4-Chlorophenol has attracted wealth of publications due to its direct relevance to environment and informative photochemical behaviours [18–20]. We report herein the photocatalytic decomposition of 4-chlorophenol (4CP) over ZnO particles stressing on the effect of operating variables such as catalyst doses, initial concentration, pH and inorganic anion additives on the photodegradation rate. We shall report the stable photo-formed products more specifically as addendum to the previously reported intermediates of 4-chlorophenol decomposition [21]. Even though pollutants are invariably associated with anions in most real waters, to the best of our knowledge the effect of the

* Corresponding author at: Department of Chemistry, Faculty of Science, Universiti Putra Malaysia, 43400 UPM Serdang, Selangor D.E., Malaysia.
Tel.: +60 3 89466777; fax: +60 3 89435380.
E-mail address: halim@science.upm.edu.my (A.H. Abdullah).

latter on photocatalytic degradation of 4-chlorophenol has not been investigated.

2. Materials and methods

2.1. Materials

4-Chlorophenol (98% pure) was obtained from Fluka Chimie, Switzerland. Solutions were prepared by using desired amount of 4-chlorophenol in deionised distilled water. ZnO (99%, Merck)) was used without further preparation for all adsorption and photocatalytic experiments. The ZnO has a surface area of $3.28\,m^2\,g^{-1}$ measured by static BET using Thermo Finnigan Sorptomatic 1990 Series analyser. The particle size of ZnO recorded on Nanophox facility was 0.4–0.5 μm. Band gap measured using PerkinElmer Lambda 35 UV/vis/NIR was 3.02 eV. HPLC grade solvents were used in the analytical determinations. Chemical standards include $Zn(NO_3)_2$ from ChemPur, hydroquinone from Ajax Chemicals, phenol from Merck, benzoquinone from ACROS Organics, catechol from BDH, Na_2HPO_4 from Fischer Chemicals, $Na_2S_2O_8$ from BDH.

2.2. Photocatalytic experiments

All experiments were carried out in an immersion well photoreactor (Fig. 1). The photoreactor is made of 300 mm long cylindrical stainless steel, having a diameter of 80 mm and effective volume of 1.19 L. The light source was a 6 W (New York Spectronics) UV lamp having irradiation density peaking at 365 nm. The photoreactor was maintained at controlled temperature of 299 K. In a typical experiment, 1 L solution constituting of the appropriate amounts of 4-chlorophenol and ZnO photocatalyst was added to the photoreactor. Where required, pH adjustment was done using equimolar NaOH and H_2SO_4 solutions. The solution was stirred for 5 min at speed of 195 rpm to attain adsorption equilibrium before irradiation. During equilibration and photocatalytic degradation, reaction solution was constantly aerated at the rate of $2\,L\,min^{-1}$. Aliquots of 20 mL of test samples were let out of the sampling tap at periodic intervals of time. ZnO was immediately filtered out using through 0.45 μm cellulose nitrate filter. The reaction progress was followed by measuring the concentration of filtrates at different irradiation times using Shimadzu model UV-1650 PC UV–vis spectrophotometer.

2.3. Analytical determinations

The pH of all test samples was measured using calibrated Radiometer PHM 201 pH meter. ICP-OES (PerkinElmer) was used to estimate the dissolution of ZnO in the course of photoreaction. Standard solutions bracketing the Zn^{2+} content of samples were prepared and run at the same time as the test samples.

The conversion of 4CP was chromatographed by Waters HPLC and Acquity UPLC fitted with Ascentis RP-C_{18} column (25 cm × 4.6 mm × 5 μm) and Acquity BEH phenyl C_{18} column (10 cm × 2.1 mm × 1.7 μm) respectively. The detection wavelength used was 280 nm. Methanol–water mobile phase in the ratio of 60–40% (v/v) was used for HPLC (isocratic) elution at flow rate of $1\,mL\,min^{-1}$. 25 mL of each test sample filtrate was extracted three times using 25 mL of diethyl ether in order to determine the intermediate product. The extract was dried with anhydrous Na_2SO_4 and concentrated under stream of nitrogen. The structural determination of intermediates was done using Shimadzu's GCMS-QP5050A operated in DI mode. BPX-5 capillary column (30 m × 0.25 mm × 0.25 μm) was used for separation. Carrier gas was helium. The column was initially maintained at 70 °C for 2 min followed by temperature increase at the rate of 10 °C min^{-1} up to 310 °C. The injector and detector temperatures were fixed at 300 and 320 °C respectively.

2.4. Multivariate experimental design

Multivariate experimental design was performed according to response surface modelling methods [22,23]. The design factors investigated were the analytical doses (g L^{-1}) of ZnO and 4CP concentration. Other design factors such as stirring rate, temperature, light intensity and oxygen supply were held constant. The number of experiments carried out in the design was guided by the formula $N = 2^n + 2n + 3$, where N is the number of experiments and n is the number of factors studied.

3. Results and discussion

3.1. Preliminary analysis

In order to validate the removal route of 4CP, the role of photolysis (UV/4CP) and adsorption (ZnO/4CP) was assessed and compared with photocatalysis (UV/ZnO/4CP). The plot of concentration of 4CP as a function of time showed no noticeable change in the concentration 4CP over 300 min except for photocatalysis (Fig. 2). 4CP was completely degraded by photocatalytic process in 180 min. Fig. 3 shows the UV–vis spectral changes during the photodegradation process. The diminution of the band peak to baseline level shows that the photodecomposition of 4CP is deemed complete.

3.2. Optimisation of 4CP decomposition

3.2.1. Central composite and response surface methodology

Multivariate experimental design delivers desirable information on the appropriate operating conditions with minimum experimental effort [24–26]. In this study, a 2^2 central composite design was employed to fit response surface of 4CP. The central composite layout consists of three sets of points: centre points, axial points
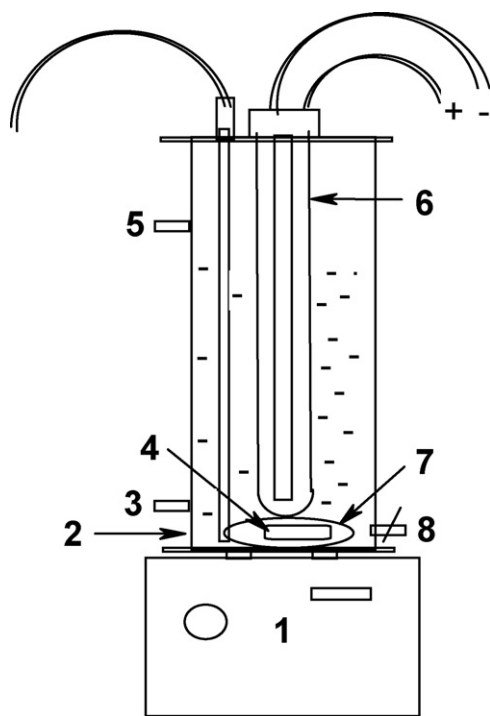
Fig. 1. Schematic view of the immersion photoreactor. (1) Magnetic stirrer with speed controller, (2) temperature controlled jacket, (3) cooling water inlet, (4) magnetic bar, (5) cooling water outlet, (6) 6 W UV lamp jacketed in quartz, (7) air draft tube and (8) sampling port.
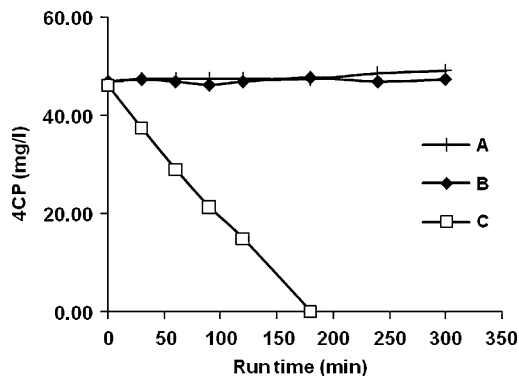
Fig. 2. Time-course profile of 50 mg L^{-1} 4CP subject to (A) adsorption on 2 g of ZnO in the dark (B) photolysis and (C) irradiation in the presence of 2 g ZnO. Initial pH 7.1–7.5.
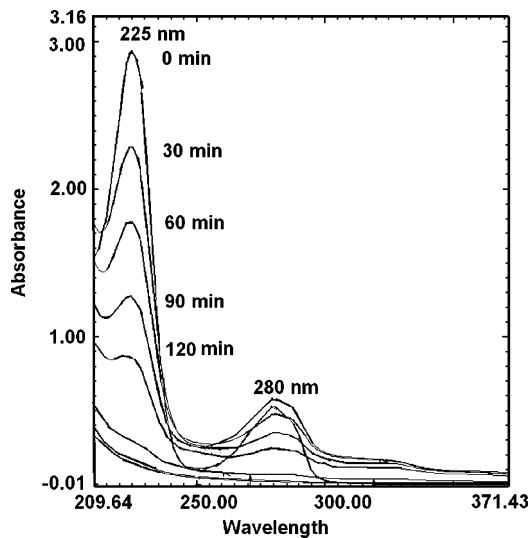
Fig. 3. UV–vis absorption spectra depicting the degradation profile of 4-chlorophenol. Initial conditions: 50 mg L^{-1}, 2 g ZnO catalyst, pH 7.5.

and factorial points. The low and high values of the factors under investigation were normalised to unity and coded as −1 and +1. Table 1 shows the actual operating variables used in the study and their coded levels. The factorial points are located at the vertices of a square having coordinates which are combinations of −1 and +1. The central values were coded as 0. The coordinates of the centre points are 0.0. Star point points were augmented to the factorial at a distance ±α = 1.41 along the centrepoint so as to make the design rotatable. Both actual values and codified levels of factors were assigned on the central composite layout (as shown in Fig. 4). The values in parentheses correspond to [ZnO] and [4CP] respectively for a given experiment. Their corresponding codes were displayed at an adjacent position. The experimental design reported here depicts 11 experiments. Four experiments were carried out at the star points as well as the factorial points. Three of the experiments replications carried out at the central point to provide an estima-

Table 1
Actual values and coded levels of operating variables.

Factor	Coded levels				
	−Alpha −1.41	Low −1	Middle 0	High +1	+Alpha +1.41
[ZnO] g L^{-1}	1.00	1.50	2.00	2.50	3.00
[4CP] g L^{-1}	0.01	0.03	0.05	0.07	0.10
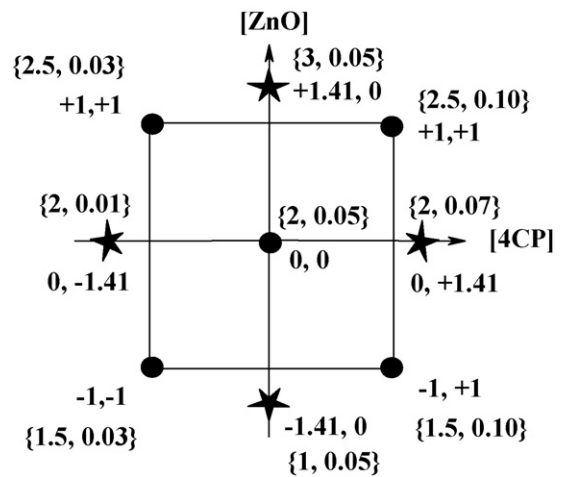
Fig. 4. Two factors central composite design used in the 4CP study.

tion of pure error and to evaluate the aptness of the response model. The experimental response factor Y_{exp} was the percentage of 4CP decomposed after 60 min of illumination. Y_{exp} was calculated by using Eq. (1).

$$Y_{exp} = \frac{1}{[4CP]_o} \times [[4CP]_o - [4CP]_t] \times 100 \qquad (1)$$

$$Y_{exp} = 39.91(\pm 2.45) + 2.89(\pm 2.87)[ZnO] - 18.33(\pm 2.87)\ [4CP] \qquad (2)$$

Response data were analysed using Stat-ease Design Expert program. The measured and predicted responses achieved in this study are shown in Table 2. The response function of 4CP is best described by the first degree polynomial model shown in Eq. (2). Each coefficient of a variable in the equation estimates the change in mean response per unit increase in the associated independent variable when the other variable is held constant. The standard error associated with the mean response and the partial regression coefficients of the equation is enclosed in the parenthesis. Analysis of variance indicated significance of all the model terms (p-value $\ll 0.05$). Fig. 5 shows the response surface plot of 4CP with observations scattered about the experimental region. The response plots were generated by keeping one factor constant at the centrepoint and varying other factors. The nature of the response surface was planar which indicates the absence of interaction of the study variables on the response function. This observation is supported by the absence of interaction term in Eq. (2) and parallel nature of response contours. The distribution of observations on the response surface plot
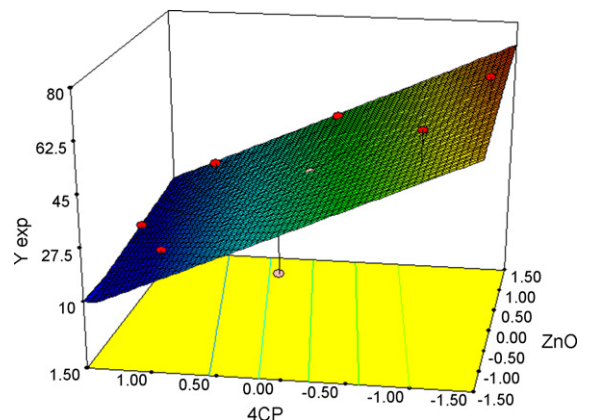
Fig. 5. Fitted surface for 4CP decomposition constructed 60 min after illumination.

Table 2
Codified variable levels from the central composite layout and responses for 4CP degradation.

Run no.	Level of variables and codes		Response after 60 min, Y_{exp} (%)	
	[ZnO] g L^{-1}	[4CP] mg L^{-1}	Measured	Predicted
1	2.50 (+1)	100 (+1)	29	24
2	1.50 (−1)	70 (+1)	22	19
3	2.50 (+1)	30 (−1)	51	61
4	1.50 (−1)	30 (−1)	66	55
5	3.00 (+1.41)	50 (0)	44	44
6	1.00 (−1.41)	50 (0)	22	36*
7	2.00 (0)	50 (0)	39	40
8	2.00 (0)	50 (0)	37	40
9	2.00 (0)	50 (0)	38	40
10	2.00 (0)	10 (−1.41)	74	66
11	2.00 (0)	100 (+1.41)	17	14

* The value exceeds diagnostic limits.

portrays three scenarios around the centrepoint (i) low response for excessive amount of either 4CP or ZnO (ii) high response with very low [4CP] and exceedingly high [ZnO] (iii) moderate [4CP] and very high [ZnO]. For economic process these combinations may be undesirable. It is evident from the response surface that the optimum operability would be consistent with 50 mg L^{-1} 4CP and 2 g ZnO.

3.2.2. Conventional experimental validation

The effect of ZnO loading on the overall decomposition rate was studied at initial 4CP concentration of 50, 70 and 100 mg L^{-1}. The ZnO load was varied for each of the initial 4CP concentration holding all other experimental conditions identical. Fig. 6 shows that as the photocatalyst amount is increased there is enhancement in photoremoval due to ready availability of total surface area and active sites of the photocatalyst. A reduction in reaction rate was generally observed at photocatalyst overdose due to opacity caused by excess photocatalyst clusters. The presence of these clusters reduces the UV penetration and at the same time increases the scattering effect. It can be concluded that the optimum amount of photocatalyst is dependent on the concentration of the substrate. The optimal solution for 4CP decomposition would therefore correspond to 2 g of ZnO and 50 mg L^{-1} of 4CP since the highest removal rate was obtained at these values.

The influence of substrate concentration on the initial rate of degradation was investigated for a wide range of initial concentration at fixed catalyst dosage of 1, 1.5 and 2 g. A graphical representation of the effect of substrate concentration on the photodestruction rate is shown in Fig. 7. The following explanations may be considered. First, at low ZnO dosage (1 g) the photodecomposition rate decreased with rise in concentration up to 50 mg L^{-1}. This may be as a result of the growing inadequacy of the number of catalytic sites. Beyond 50 mg L^{-1} the degradation rate was nearly

constant. Secondly, by keeping the photocatalyst dose at 1.5 and 2 g L^{-1} and varying the 4CP concentrations reaction rate increased at the initial stage due to the ready availability of catalytic sites of the ZnO. However, as initial concentrations exceed 50 mg L^{-1} the rate of degradation decreased because the active sites of the photocatalyst were tightly occupied. Another factor which may be responsible for the drop in photocatalytic degradation rate is the competition between 4CP and hydroxyl ions for surface-trapped photogenerated holes. Hence, the optimal 4CP concentration for photodegradation is confirmed to be 50 mg L^{-1}.

3.3. Photocatalytic kinetics

The degradation of 4CP under the experimental conditions of the study agreed remarkably with the zero-order kinetics. Generally speaking, the rate law for degradation of 4CP may be represented by the Eq. (3). Accordingly, the integrated zero-order rate law may take the form (4).

$$\frac{-d[4CP]}{dt} = k \tag{3}$$

$$[4CP]_t = -kt + [4CP]_o \tag{4}$$

where $[4CP]_t$ and $[4CP]_o$ is the concentration of 4CP (M, mol L^{-1} or ppm) at time t and when $t = 0$ respectively and k is the pseudo zero-order constant (usually expressed as M s^{-1}, mol L^{-1} s or ppm s^{-1}). A plot of [4CP] versus t would give a straight line with slope $= -k$ and intercept $= [4CP]_o$. The applicability of the zero-order kinetics to this study has been confirmed by the linearity of the plot of [4CP] against irradiation time for various experiments (Fig. 8) with R-square value > 0.99.

Fig. 6. Observed influence of catalyst concentration on degradation rate. Initial 4CP concentration range = 50–100 mg L^{-1}; catalyst load = 0.5–3 g; pH ∼ 7.5.
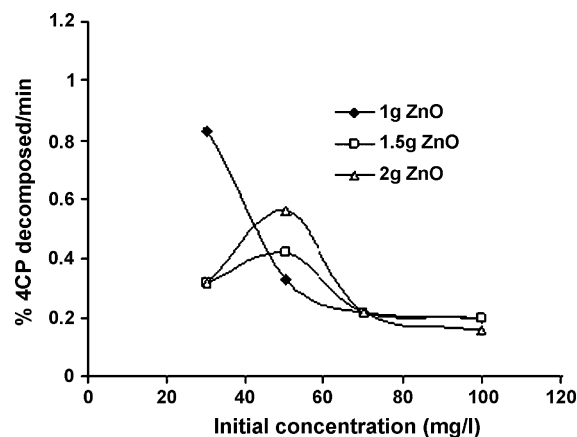
Fig. 7. Effect of substrate initial concentration at different catalyst loading on initial rate of degradation. 4CP concentration range = 30–100 mg L^{-1}; catalyst load = 1–2 g; pH 7.1–7.9.
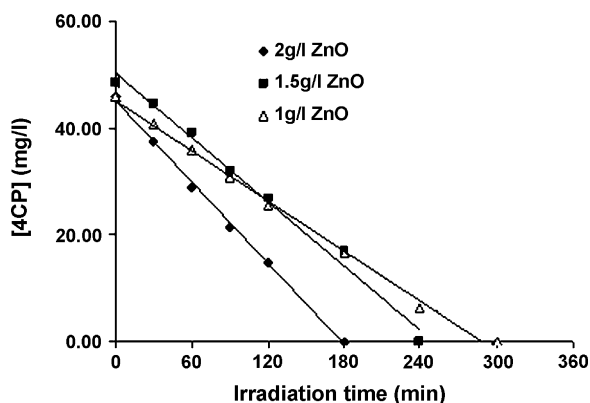
Fig. 8. Zero-order rate graph of 4CP degradation. Initial conditions: $50\,mg\,L^{-1}$ 4CP; ZnO = 1 g, 1.5 g or 2 g (as appropriate); pH range 7.2–7.7.

3.4. Photocorrosion of ZnO surface

Since ZnO is susceptible to dissolution it is imperative to know the amount of zinc ion left in the decontaminated water. ZnO dissolution data collected on ICP-OES indicated little ZnO loss under irradiation. The initial pH during the test averaged 7.54 with mean deviation of ±0.17. The dissolution observed is mostly low (<0.02%) and does not increase appreciably with irradiation time.

3.5. Influence of solution pH on photomineralisation rate

The effect of pH of reaction solution on photo-oxidation rate was studied at pH of ca. 4–10. Reactivity solutions were adjusted to initial pH of 4, 6, 7, 9 and 10. Fig. 9 shows a comparison of photodecomposition rate at various pH values. As observed, the photocatalytic reaction of 4CP is inhibited at pH 4 which may be due to substantial loss of ZnO at exceedingly low pH in accord with Eq. (5). The degradation rate increases up to pH 6 as ZnO stability is less disturbed (see Eq. (6)). There is imperceptible change in degradation rate between pH 6 and 7. Beyond pH 7 there is substantial enhancement in the degradation rate. The maximum degradation efficiency in this study was attained at pH 9.

$$ZnO + 2H^+ \rightarrow Zn^{2+} + H_2O \qquad \text{(acidic dissolution)} \qquad (5)$$

$$phOH(Cl) \underset{H^+}{\overset{OH^-}{\rightleftharpoons}} (Cl)phO^- \qquad (6)$$
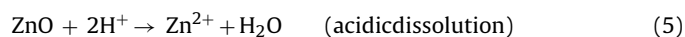
The 4CP photodecomposition rate was nearly constant between the pH_{pzc} and pH 10. A priori aqueous ZnO is largely in hydrolysed form or 'zinc-ol' as shown in Eq. (7). Since in the update by Kosmulski [27] ZnO has been reported to possess the point of zero charge of 9 zinc-ol group would be protonated to $ZnOH_2^+$ below pH_{pzc} or deprotonated to $Zn–O^-$ as pH_{pzc} is exceeded. Thus, at pH
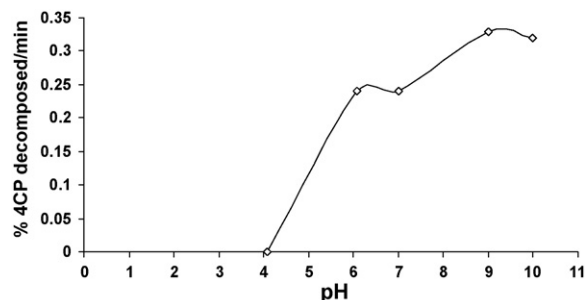
Fig. 9. Variation of decomposition rate with pH. Initial 4CP concentration = $50\,mg\,L^{-1}$, ZnO = 2 g.

10 the negatively charged ZnO surface and the high concentration of phenoxide above the pK_a value of 4CP (9.38) may result in electrostatic repulsion which cannot be overcome by the low enthalpy possessed by ZnO active sites thereby leading to decreased rate. Moreover, the stability of ZnO may not be guaranteed at this high pH due to possibility of alkaline dissolution of ZnO (shown in Eq. (8)).

$$ZnO + H_2O \rightarrow \;\equiv Zn–OH + OH^- \qquad (7)$$

$$ZnO + H_2O + 2OH^- \rightarrow [Zn(OH)_2]^{2+} \quad \text{(alkaline dissolution)} \quad (8)$$
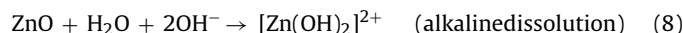
3.6. Effect of additives on 4CP decomposition rate

Since real waters usually contain inorganic ions coexisting with organic pollutants the effect of inorganic anions on reaction rate was studied at levels of $0.4\,mg\,L^{-1}$. The inorganic ions investigated include HPO_4^{2-}, SO_4^{2-}, Cl^- and $S_2O_8^{2-}$ added as sodium salts. The % 4CP removal in ion free solution at pH 7 was 71%. Initial solution pH was adjusted to 7 so as to establish a standard for comparison. Photoremoval rate was enhanced by the presence of inorganic anions in the order Cl^- (74%) < SO_4^{2-} (96%), $S_2O_8^{2-}$ (96%). The photocatalytic reaction was totally inhibited by HPO_4^{2-} due to strong binding of the anion to the active sites thereby preventing the adsorption of 4CP. The enhancement of decomposition rate by sulphate and peroxodisulphate ions is may be linked to the direct or indirect formation of $SO_4^{\bullet-}$ chemically shown by Eqs. (9)–(12). Previous literature has shown that this in situ generated radical can sufficiently act as strong oxidising agent or initiate the formation of hydroxyl radical [28,29].

$$S_2O_8^{2-} + e_{CB}^- \rightarrow SO_4^{2-} + SO_4^{\bullet-} \qquad (9)$$

$$SO_4^{2-} + {}^\bullet OH \rightarrow SO_4^\bullet + OH^- \qquad (10)$$

$$SO_4^{2-} + h^+ \rightarrow SO_4^{\bullet-} \qquad (11)$$

$$SO_4^{\bullet-} + H_2O \rightarrow SO_4^{2-} + {}^\bullet OH + H^+ \qquad (12)$$
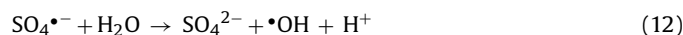
Usually Cl^- has been reported to retard photodegradation rate. In contrast, our results showed a slight increase in the rate of 4CP transformation. It is worth noting that the inhibitive effect of Cl^- ion is favoured by acidic pH since this anion would adsorb strongly onto the surface of the semiconductor particles thereby hindering the pollutant [29]. Since our initial working environment was neutral this effect was not observed. Lair et al. [30] reported increase in photocatalytic oxidation rate of naphthalene degradation by chloride ions attributed it to substrate loss through volatilisation of 4CP caused by rise in ionic strength. However, Wiszniowski et al. [31] have shown that the addition of Cl^- at pH > 7 did not have any influence on the mineralisation of humic acid. At any rate, the enhancement of decomposition rate by Cl^- and SO_4^{2-} will be most welcome as they are among the commonest anions in open waters.

3.7. Photoproducts and mineralisation

The photocatalytic 4CP degradation yielded catechol, phenol, 4-chlorocatechol and hydroquinone as pathway products. These products were identified by GC–MS and chromatographic comparison with external standards. Table 3 shows the retention times of the detected compounds at natural pH. To the best of our knowledge, we are reporting catechol for the first time in the photocatalytic degradation of 4CP. All other photoproducts determined were reported previously in 4CP decomposition either by photolysis or photocatalysis [32,33]. The degradation of $70\,mg\,L^{-1}$ 4CP was recorded on UHPLC. Fig. 10(A) shows the UHPLC peaks of phenolics detected after 180 min of irradiation. Hydroquinone, 4-chlorocatechol and 4-chlorophenol emerged on the UHPLC at retention times of 0.7, 1.2 and 1.7. The amount of

Table 3
Retention times of detected photoproducts.

Photoproduct	Retention times on HPLC		
	Experiment	External standard	GC–MS
Hydroquinone	2.9/3.1	2.9	Detected
Catechol	4.0	4.1	–
Phenol	6.1	4.4	Detected
4-Chlorocatechol	9.7	n.a.	Detected
4-Chlorophenol	15.4	15.5	Detected
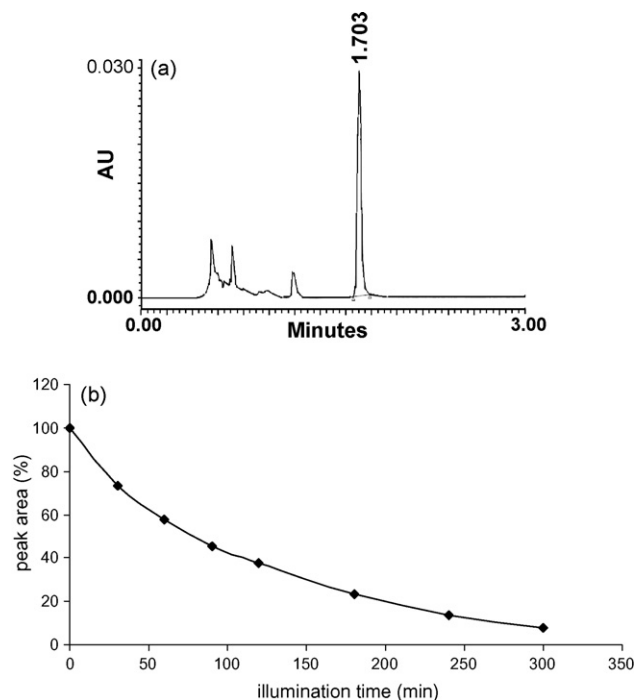
Fig. 10. (A) UPLC chromatogram showing the chromatographic peak of 4CP (major) and intermediate products. UPLC parameters: Injection volume = 2 μL; run time = 3 min; detection wavelength = 280 nm; detector = PDA. (B) Changes in peak area recorded on UPLC during photomineralisation process. Initial conditions: 70 mg L^{-1} 4CP, 1 g ZnO; pH 7.2.

4CP has been reduced to 18 mg L^{-1}. The depletion of 70 mg L^{-1} 4CP during 300 min of photomineralisation process is shown by the time-course plot of % peak area recorded on UPLC (Fig. 10(B)). It was observed that about 6 mg L^{-1} 4CP is left in solution after 300 min. Also, a high amount of undecomposed intermediates are categorically readable from the chromatograms. Conversely, at optimum experimental levels of ZnO and 4CP the mineralisation of 4CP was confirmed by using HPLC. An inspection of HPLC peaks shows that maximum level of the photoproducts was attained in 30–60 min. The relative amounts of hydroquinone, catechol and
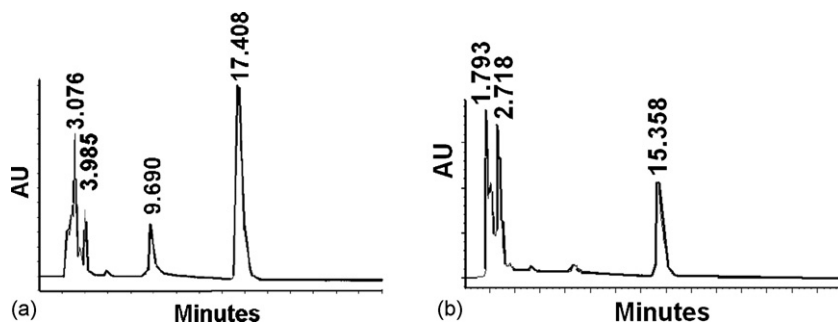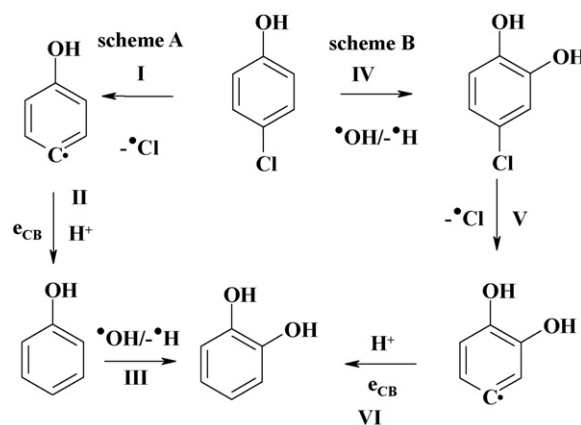
Fig. 12. A radical mechanism to account for the pathways of photoproducts in the course of mineralisation. Initial conditions: 50 mg L^{-1} 4CP; 2 g ZnO; pH 7.5 (natural).

4-chlorocatechol were 32, 8 and 15%. The initial growth of intermediate products and decay of 4CP peak can be seen from sample chromatograms in Fig. 11. After 300 min chromatograms indicated no traces of 4-chlorophenol and intermediates in the solution.

3.8. Reaction mechanism

Upon illumination of aqueous semiconductor particles with light of sufficient energy, charge separation is induced resulting in the formation of valence band holes and conduction band electrons. These charge carriers may participate in the formation of active oxidising species such as hydroxyl radical, hydroperoxyl radical, hydrogen peroxide and superoxide [34]. Several literatures attributed the oxidation of organic compounds mainly to positive hole and/or hydroxyl radical [35,36]. Based on quantum yield study the oxidative mechanism over semiconductor ought to proceed via positive hole [37]. However, there are convincing experimental proofs that both valence band hole and hydroxyl radical are involved in oxidative conversions on semiconductor photocatalysts [19,38]. More specifically, hydroxyl radical has been shown to be the major oxidant involved in 70–90% of the photo-oxidation of organic compounds notably chlorophenols [36,39]. In order not to depart from these conclusions and the fact that hydroxylated products are reported in this study, hydroxyl radical mechanism is employed to explain the photo-oxidation mechanism.

Since the phenolic ring is labile to hydroxyl radical attack at various positions many mechanistic pathways can be described to account for the products of 4CP oxidation. In this report, we would limit our mechanism to catechol which is a new intermediate. Fig. 12 shows a mechanistic scheme to account for the formation of catechol. It has been established that the first process in 4CP photo-oxidation involves the scission of C–Cl bond [40,41]. Primarily, if 4CP is homolysed at ring-Cl bond a short-lived hydroxyphenyl

Fig. 11. HPLC chromatograms depicting eluted peaks at different reaction times (A) 30 min (B) 90 min. Initial conditions: 50 mg L^{-1} 4CP; 2 g ZnO; pH 7.5.

radical (HPR) is formed (Eq. (1)). This organic radical may combine with proton to form phenol (Eq. (2)). Evidence for the formation of HPR has been provided by Lipczynska-Kochany et al. [42]. Probably catechol is formed by o-hydroxylation of phenol (Eq. (3)). If 4CP is hydroxylated at the ortho position (scheme B, Fig. 9) 4-chlorocatechol is formed (Eq. (4)). The *para*-dechlorination of 4-chlorocatechol yields 1,2-dihydroxyphenyl radical (1,2-diHPR; Eq. (5)). In a similar way to HPR (vide supra) the 1,2-diHPR radical can also combine with proton in the presence of conduction band electron to form catechol (Eq. (6)). The subsequent processes that lead to mineralisation of 4CP have been highlighted by Theurich et al. [33] in a study of the degradation of 4CP over TiO_2. Further oxidative hydroxylation of catechol and phenol gives hydroxyhydroquinone and hydroquinone. Subsequently, hydroquinone and hydroxyhydroquinone are converted to benzoquinone hydroxybenzoquinone. Finally, quinone rings are opened to form aliphatic compounds which upon further oxidation are mineralised to CO_2 and H_2O.

4. Conclusions

- Optimal degradation solution corresponds to $50\,\mathrm{mg\,L^{-1}}$ 4CP and 2 g ZnO respectively.
- The photo-oxidative degradation of 4CP under the experimental conditions of the study follows essentially the zero-order kinetics. Maximum degradation rate was attained at mild basic environment.
- The degradation was more favourable in the mild alkaline range with maximum rate at pH 9.
- Inorganic anions such as Cl^-, $SO_4{}^{2-}$ and $S_2O_8{}^{2-}$ enhanced photomineralisation rate of 4CP whereas $HPO_4{}^{2-}$ hampered the process.
- The stable products identified during the degradation process at natural initial pH environment are catechol, phenol, 4-chlorocatechol and hydroquinone. The mechanism for the formation of catechol is proposed.

Acknowledgements

References

[1] K. Orloff, H. Falk, An international perspective on hazardous waste practices, Int. J. Hyg. Environ. Health 206 (2003) 291–302.
[2] Mc. Pera-Titus, V. García-Molina, M.A. Baños, J. Giménez, S. Esplugas, Degradation of chlorophenols by means of advanced oxidation processes: a general review, Appl. Catal. B: Environ. 47 (2004) 219–256.
[3] B.F. Abramović, V.B. Anderluh, A.S. Topalov, F.F. Gaál, Kinetics of photocatalytic removal of 2-amino-5-chloropyridine from water, APTEFF 35 (2004) 1–280.
[4] E. Pelizzetti, V. Maurino, C. Minero, V. Carlin, E. Pramauro, O. Zerbinati, M.L. Tosato, Photocatalytic degradation of atrazine and other s-triazine herbicides, Environ. Sci. Technol. 24 (1990) 1559–1565.
[5] A. Fujishima, T.N. Rao, D.A. Tryk, Titanium dioxide photocatalysis, J. Photochem. Photobiol. C: Photochem. Rev. 1 (2000) 1–21.
[6] O. Carp, C.L. Huisman, A. Reller, Photoinduced reactivity of titanium dioxide, Prog. Solid State Chem. 32 (2004) 33–177.
[7] V.H. Grasian, Environmental catalysis, CRC Press, Taylor and Francis Group, New York, 2005.
[8] Z. Zainal, L.K. Hui, M.Z. Hussein, Y.H. Taufiq-Yap, A.H. Abdullah, I. Ramli, Removal of dyes using immobilized titanium dioxide illuminated by fluorescent lamps, J. Hazard. Mater. B 125 (2005) 113–120.
[9] N. Daneshvar, D. Salari, A.R. Khataee, Photocatalytic degradation of azo dye acid red 14 in water on ZnO as an alternative catalyst to TiO_2, J. Photochem. Photobiol. A: Chem. 162 (2004) 317–322.
[10] A. Akyol, H.C. Yatmaz, M. Bayramoglu, Photocatalytic decolorization of remazol red RR in aqueous ZnO suspensions, Appl. Catal. B: Environ. 54 (2004) 19–24.
[11] I. Poulios, D. Makri, X. Prohaska, Photocatalytic treatment of olive milling waste water: oxidation of protocatechuic acid, Global Nest: Int. J. 1 (1999) 55–62.
[12] F. Peng, H. Wang, H. Yu, S. Chen, Preparation of aluminium foil-supported nano-sized ZnO thin films and its photocatalytic degradation to phenol under visible light irradiation, Mater. Res. Bull. 41 (2006) 2123–2129.
[13] T. Ivanciuc, O. Ivanciuc, D.J. Klein, Prediction of environmental properties for chlorophenols with posetic quantitative super-structure/property relationships (QSSPR), Int. J. Mol. Sci. 7 (2006) 358–374.
[14] F.J. Benitez, J. Beltran-Heredia, J.L. Acero, F.J. Rubio, Contribution of free radicals to chlorophenols decomposition by several advanced oxidation processes, Chemosphere 41 (2000) 1271–1277.
[15] C.-J. Liao, T.-L. Chung, W.-L. Chen, S.-L. Kuo, Treatment of pentachlorophenol-contaminated soil using nano-scale zero-valent iron with hydrogen peroxide, J. Mol. Catal. A: Chem. 265 (2007) 189–194.
[16] R.J. Lewis Sr., Hazardous Chemicals Desk Reference, fifth ed., John Wiley and Sons, New York, 2002.
[17] R.P. Pohanish, S.A. Greene, Hazardous Material Handbook, Van Nostrand Reinhold/International Thompson Publishing, New York, 1996.
[18] K. Vinodgopal, U. Stafford, K.A. Gray, P.V. Kamat, Electrochemically assisted photocatalysis 2. The role of oxygen and reaction intermediates in the degradation of 4-chlorophenol on immobilized TiO_2 particulate films, J. Phys. Chem. 98 (1994) 6797–6803.
[19] U. Stafford, K.A. Gray, P.V. Kamat, Radiolytic and TiO_2-assisted photocatalytic degradation of 4-chlorophenol: a comparative study, J. Phys. Chem. 98 (1994) 6343–6351.
[20] J. Krýsa, G. Waldner, H. Měšťánková, J. Jirkovský, G. Grabner, Photocatalytic degradation of model organic pollutants on an immobilized particulate TiO_2 layer: roles of adsorption processes mechanistic complexity, Appl. Catal. B: Environ. 64 (2006) 290–301.
[21] T. Sehili, P. Boule, J. Lemaire, Photocatalysed transformation of chloroaromatic derivatives on zinc oxide III: chlorophenols, J. Photochem. Photobiol. A: Chem. 50 (1989) 117–127.
[22] R.G. Brereton, Applied Chemometrics for Scientists, John Wiley and Sons, 2007.
[23] R.L. Mason, R.F. Gunst, J.L. Hess, Statistical Design and Analysis of Experiments, John Wiley and Sons Inc., 1989.
[24] P. Gemperline, Practical Guide to Chemometrics, second ed., CRC Press, Taylor and Francis Group, 2006.
[25] J. Anthony, Design of Experiments for Engineers and Scientists, Elsevier Science and Technology Books, 2003.
[26] J. Neter, W. Wasserman, M.H. Kutner, Applied Statistics, third ed., Irwin Inc., 1989.
[27] M. Kosmulski, pH-dependent surface charging and points of zero charge III. Update, J. Colloid Interf. Sci. 298 (2006) 730–741.
[28] L. Ravichandran, K. Selvam, M. Swaminathan, Effect of oxidants and metal ions on photodefluoridation of pentafluorobenzoic acid with ZnO, Sep. Purif. Technol. 56 (2007) 192–198.
[29] K.-H. Wang, Y.-H. Hsieh, M.-Y. Chou, C.-Y. Chang, Photocatalytic degradation of 2-chloro and 2-nitrophenol by titanium dioxide suspensions in aqueous solution, Appl. Catal. B: Environ. 21 (1999) 1–8.
[30] A. Lair, C. Ferronato, J.-M. Chovelon, J.-M. Herrmann, Naphthalene degradation in water by heterogeneous photocatalysis: an investigation of the influence of inorganic anions, J. Photochem. Photobiol. A: Chem. 193 (2008) 193–203.
[31] J. Wiszniowski, D. Robert, J. Surmacz-Gorska, K. Miksch, J.-V. Weber, Photocatalytic mineralization of humic acids with TiO_2: effect of pH, sulfate and chloride anions, Int. J. Photoenergy 5 (2003) 69–74.
[32] M. Czaplicka, Photo-degradation of chlorophenols in the aqueous solution, J. Hazard. Mater. B134 (2006) 45–59.
[33] J. Theurich, M. Lindner, D.W. Bahnemann, Photocatalytic degradation of 4-chlorophenol in aerated aqueous titanium dioxide suspensions: a kinetic and mechanistic study, Langmuir 12 (1996) 6368–6376.
[34] U.I. Gaya, A.H. Abdullah, Heterogeneous photocatalytic degradation of organic contaminants over titanium dioxide: a review of fundamentals, progress and problems, J. Photochem. Photobiol. C: Rev. 9 (2008) 1–12.
[35] M.R. Hoffmann, S.T. Martin, W. Choi, D.W. Bahnemann, Environmental applications of semiconductor photocatalysis, Chem. Rev. 95 (1995) 69–96.
[36] C. Richard, P. Boule, Oxidising species involved in transformations on zinc oxide, J. Photochem. Photobiol. A: Chem. 60 (1991) 235–243.
[37] K. Ishibashi, A. Fujishima, T. Watanabe, K. Hashimoto, Quantum yields of active oxidative species formed on TiO_2 photocatalyst, J. Photochem. Photobiol. A: Chem. 134 (2000) 139–142.
[38] C. Richard, Regioselectivity of oxidation by positive holes (h+) in photocatalytic aqueous transformations, J. Photochem. Photobiol. A: Chem. 72 (1993) 179–182.
[39] T. Sehili, Photocatalysed transformation of chloroaromatic derivatives on zinc oxide IV: 2,4-dichlorophenol, Chemosphere 22 (1991) 1053–1062.
[40] A-P.Y. Durand, R.G. Brown, Photoreactions of 4-chlorophenol in aerated and deaerated aqueous solution: use of LC-MS for photoproduct identification, Chemosphere 31 (1995) 3595–3604.
[41] P. Boule, C. Guyon, J. Lemaire, Photochemistry and environment. IV. Photochemical behavior of monochlorophenols in dilute aqueous solution, Chemosphere 11 (1982) 1179–1188.
[42] E. Lipczynska-Kochany, J. Kochany, J.R. Bolton, Electron paramagnetic resonance spin trapping detection of short-lived radical intermediates in the direct photolysis of 4-chlorophenol in aerated aqueous solution, J. Photochem. Photobiol. A: Chem. 62 (1991) 229–240.